Article

Cell Reports

Neuronal CTCF Is Necessary for Basal and Experience-Dependent Gene Regulation, Memory Formation, and Genomic Structure of *BDNF* and *Arc*

Graphical Abstract

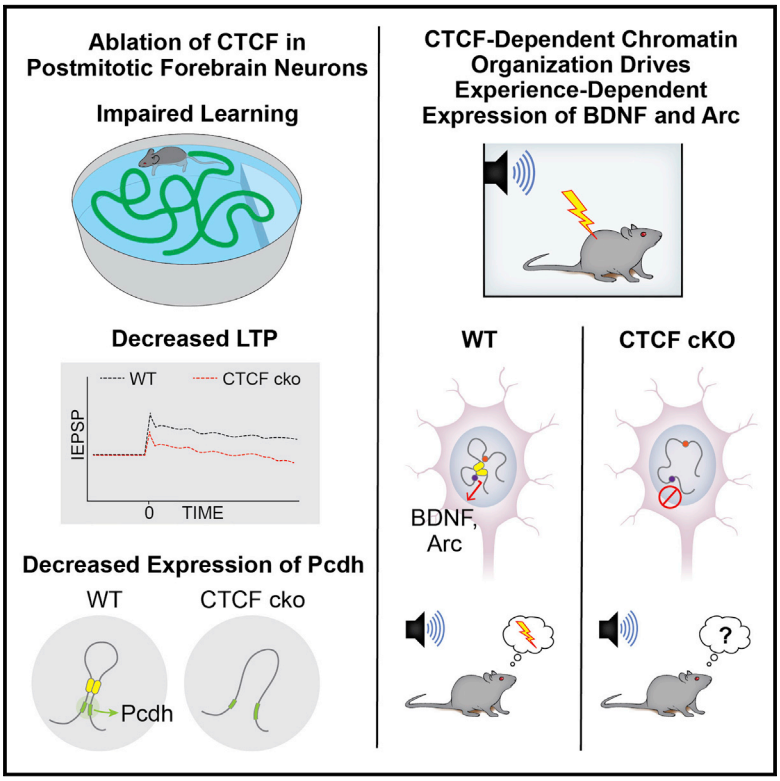

Authors

Dev Sharan Sams, Stefano Nardone, Dmitriy Getselter, ..., Hanoch Kaphzan, Ofir Hakim, Evan Elliott

Correspondence

evan.elliott@biu.ac.il

In Brief

Sams et al. examine the role of CTCF in cognitive processes in the hippocampus. Using genome-wide approaches, they find that CTCF regulates protocadherin and memory-related genes in the hippocampus. Circular chromosome confirmation capture (4C) suggests that experience-dependent upregulation of memory-related genes is related to CTCF-dependent chromatin organization.

Highlights

- Hippocampal CTCF is necessary for learning and memory
- Neuronal CTCF specifically regulates protocadherin and memory-related genes
- CTCF is mandatory for the genomic organization transcription of key learning genes

Accession Numbers

GSE84176

Sams et al., 2016, Cell Reports *17*, 2418–2430
November 22, 2016
http://dx.doi.org/10.1016/j.celrep.2016.11.004

OPEN ACCESS
CellPress

Cell Reports
Article

Neuronal CTCF Is Necessary for Basal and Experience-Dependent Gene Regulation, Memory Formation, and Genomic Structure of *BDNF* and *Arc*

Dev Sharan Sams,[1] Stefano Nardone,[1] Dmitriy Getselter,[1] Dana Raz,[2] Moran Tal,[2] Prudhvi Raj Rayi,[3] Hanoch Kaphzan,[3] Ofir Hakim,[2] and Evan Elliott[1,4,*]

[1]Faculty of Medicine, Bar Ilan University, Safed 13215, Israel
[2]The Mina and Everard Goodman Faculty of Life Sciences, Bar-Ilan University, Ramat-Gan 5290002, Israel
[3]Faculty of Natural Sciences, University of Haifa, Haifa 3498838, Israel
[4]Lead Contact
*Correspondence: evan.elliott@biu.ac.il
http://dx.doi.org/10.1016/j.celrep.2016.11.004

SUMMARY

CCCTC-binding factor (CTCF) is an organizer of higher-order chromatin structure and regulates gene expression. Genetic studies have implicated mutations in CTCF in intellectual disabilities. However, the role of CTCF-mediated chromatin structure in learning and memory is unclear. We show that depletion of CTCF in postmitotic neurons, or depletion in the hippocampus of adult mice through viral-mediated knockout, induces deficits in learning and memory. These deficits in learning and memory at the beginning of adulthood are correlated with impaired long-term potentiation and reduced spine density, with no changes in basal synaptic transmission and dendritic morphogenesis and arborization. Cognitive disabilities are associated with down-regulation of cadherin and learning-related genes. In addition, CTCF knockdown attenuates fear-conditioning-induced hippocampal gene expression of key learning genes and loss of long-range interactions at the *BDNF* and *Arc* loci. This study thus suggests that CTCF-dependent gene expression regulation and genomic organization are regulators of learning and memory.

INTRODUCTION

Epigenetic regulation of neuronal gene expression in the hippocampus plays a primary role in learning and memory (Miller et al., 2008). Epigenetics refers to covalent chromatin modifications that affect gene transcription without affecting the DNA sequence and includes DNA methylation and histone acetylation. For instance, histone deacetylases (e.g., HDAC2 and HDAC4) regulate learning and memory by modifying histone acetylation levels at learning-associated genes (Guan et al., 2009; Kim et al., 2012). Besides histone acetylation, another epigenetic marker, DNA methylation, has been demonstrated to regulate memory. Learning events increase levels of DNA methyltransferases (DNMTs) in the brain and induce methylation changes in learning-associated genes (Miller and Sweatt, 2007). While the emerging field of behavioral epigenetics has determined the importance of local epigenetic modifications in the regulation of learning-related genes, the roles of three-dimensional DNA structure and high-order genomic organization are largely unknown.

In recent years, studies have underlined the role of three-dimensional DNA structure and chromatin conformation as a primary critical regulator of gene expression patterns (Holwerda and de Laat, 2012). For example, expression of the sonic hedgehog (SHH) receptor Ptch1, and subsequent SHH-mediated handplate development, is mediated by a chromatin contact with a distant *cis*-regulatory element (Lopez-Rios et al., 2014). However, the role of three-dimensional DNA structure in mammalian behavior and brain physiology is unclear.

CCCTC-binding factor (CTCF), a major regulator of three-dimensional DNA organization, has been implicated in the genetic etiology of neurodevelopmental conditions, including intellectual disabilities, autism, and schizophrenia (Lanni et al., 2013; Juraeva et al., 2014; Gregor et al., 2013). In particular, de novo mutations in CTCF were found in individuals with intellectual disabilities (Gregor et al., 2013). A growing number of studies demonstrate that CTCF is vital for the regulation of higher-order genome structure by binding to specific genomic sites at promoters, enhancers, and borders between chromosomal loci through its zinc-finger domains (Merkenschlager and Odom 2013). CTCF can form chromosomal loops between genes and distant regulatory elements or insulate chromosomal domains. These conformational events maintain proper gene transcription levels by bringing together genes and regulatory elements and by insulating chromosomal regions with different epigenetic and transcriptional states. They also define boundaries between topological domains (TADs), which are chromosomal units of high interaction frequency (Phillips-Cremins et al., 2013; Rao et al., 2014).

Initial studies into the role of CTCF in neuronal development determined that deletion of CTCF at early developmental time points dysregulates neural progenitor proliferation, differentiation, and survival (Watson et al., 2014; Moore et al., 2012). In

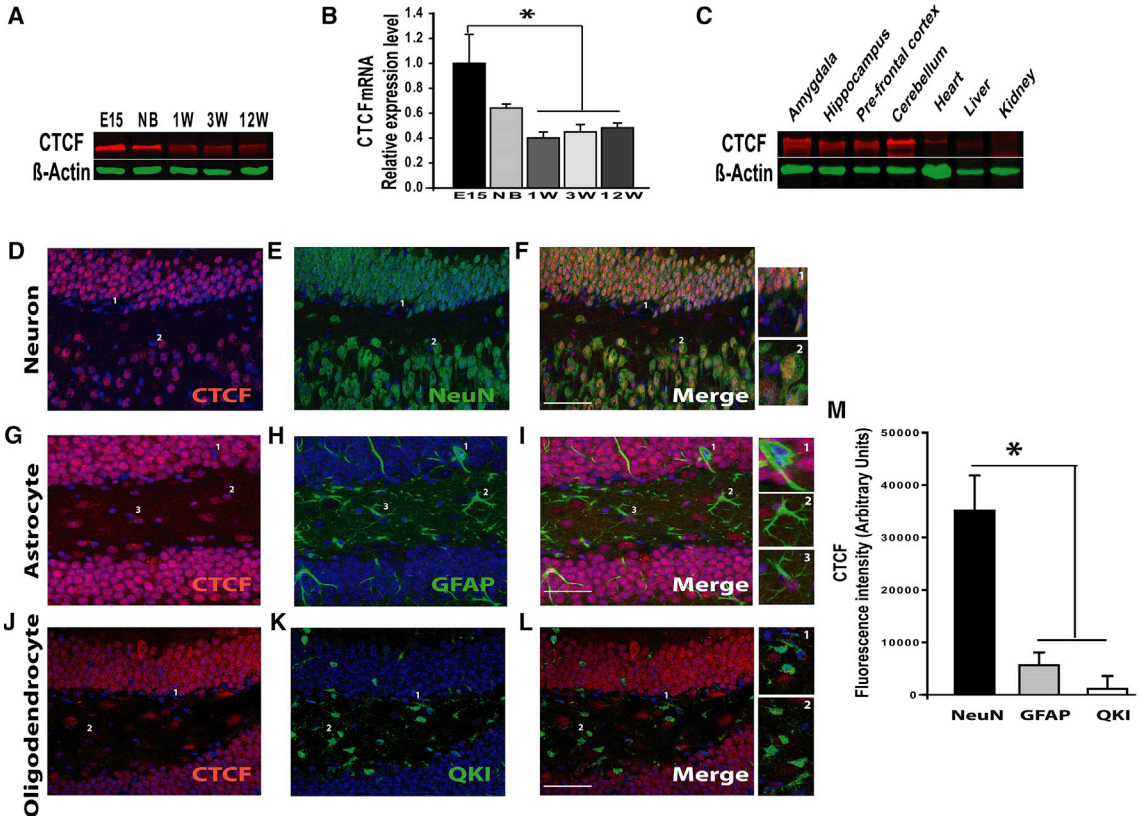

Figure 1. Spatiotemporal Expression of CTCF in the Brain and Preferential Expression in Neurons

(A and B) Western blot analysis of *CTCF* protein levels (A) and real-time PCR analysis of CTCF transcript levels (b) in the whole mouse brain during different developmental time points (embryonic day 15 [E15], newborn [NB], and postnatal week 1 [1W], 3W, and 12W). Error bars represent SEM (n = 5; $F_{1,4} = 7.332$; p = 0.001, one-way ANOVA; *p < 0.05, Tukey test).

(C) Western blot analysis of CTCF protein levels in brain and select peripheral tissues from adult mouse.

(D–L) Immunohistochemistry of mouse hippocampus (dentate gyrus) stained for CTCF (D, G, and J), neuronal marker NeuN (E), astrocyte marker GFAP (H), and oligodendrocyte marker Qki (K).

(M) CTCF fluorescence is significantly expressed in NeuN-expressing cells compared to GFAP and Qki expressing cells (n = 4; $F_{2,54} = 11.658$; p = 0.001, one-way ANOVA; *p < 0.05 Tukey test). Error bars represent SEM. Scale bar, 100 μm.

another study, deletion of CTCF in neurons of mice caused postnatal growth retardation, motor problems, and death at the age of 4 weeks, with altered expression of clustered protocadherin (*Pcdh*) genes (Hirayama et al., 2012). In addition, in vitro studies have highlighted the importance of CTCF binding for the transcription of brain-derived neurotrophic factor (*BDNF*) (Chang et al., 2010). BDNF mediates both the development and maintenance of synaptic networks and is mandatory for hippocampal-dependent memory. Together, these studies suggest that CTCF is mandatory for proper neuronal development. However, the role of CTCF in mature neuronal function, maintenance of three-dimensional DNA structure in the brain, and cognitive processes has not been determined.

In the current study, we aimed to determine the molecular role of CTCF-mediated DNA conformation in the process of learning and memory. Using conditional knockout mice and adeno-viral-mediated knockout of CTCF in the hippocampus, coupled with genome-wide gene expression and circular chromosome conformation capture (4C), we find a vital role for CTCF-mediated gene expression in the formation of hippocampal-dependent memory. These data elucidate how CTCF and DNA structure are primary components of memory-related processes in the brain.

RESULTS

Characterization of CTCF in the Mouse Brain

Initially, we characterized the temporal and spatial expression of CTCF in the mouse brain. Both CTCF mRNA transcripts and protein were detected in whole-brain extracts throughout development. Protein levels were highest during prenatal stages (embryonic day 15 [E15]) and displayed a gradual decrease throughout development (Figure 1A). A similar pattern was detected in *CTCF* gene expression during development, as detected by real-time PCR (Figure 1B). In the adult mouse, CTCF protein levels were higher in all studied brain regions than in kidney, heart, and liver (Figure 1C). Furthermore, we performed immunostaining of neurons (NeuN), astrocytes (GFAP),

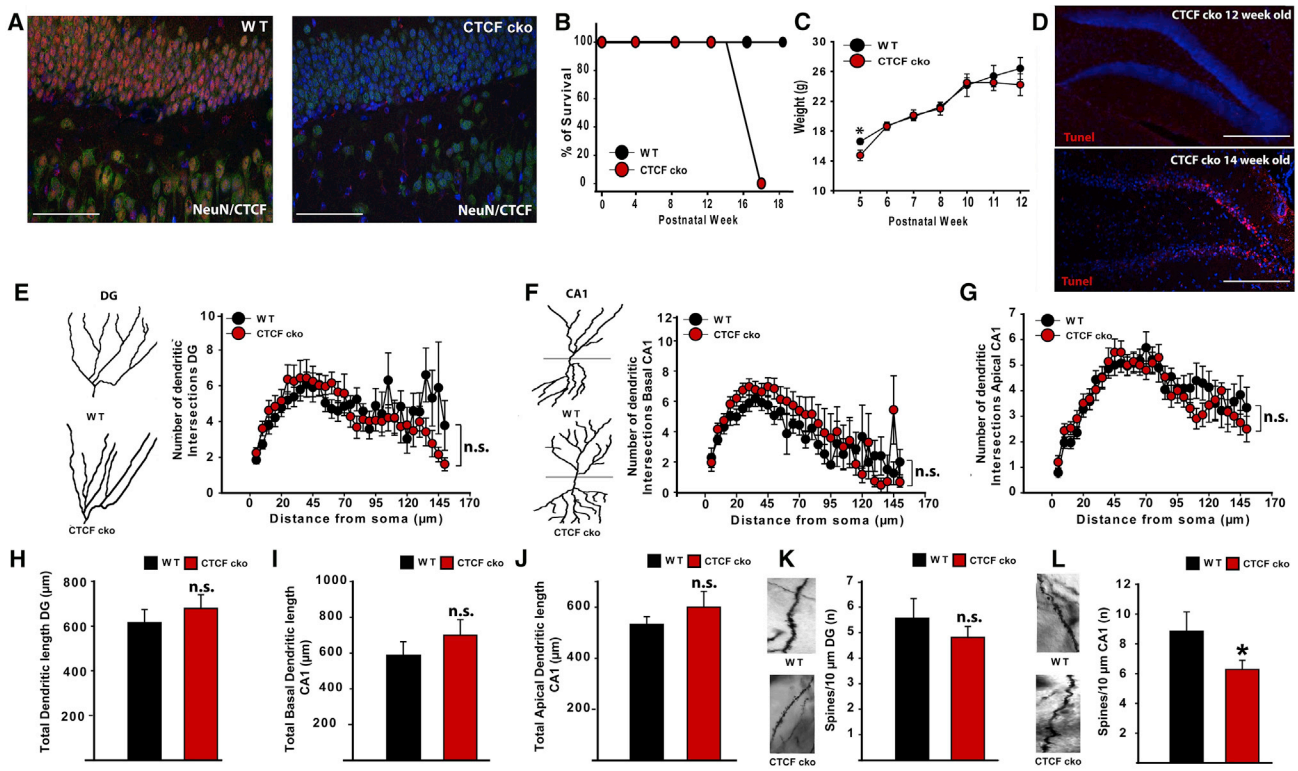

Figure 2. Characterization of Time-Point-Dependent Changes in CTCF cko Mice

(A) Immunofluorescence analysis of CTCF in the hippocampus of 8-week-old wild-type and CTCF cko mice shows depletion of CTCF from hippocampal neurons.

(B) Lifespan of CTCF cko mice.

(C) Weight of CTCF cko mice during its short lifespan (*$p < 0.05$, two-tailed t test).

(D) TUNEL analysis for apoptotic cells in the hippocampus of 12-week-old and 14-week-old CTCF cko mice. Apoptosis is detected in 14-week-old, but not 12-week-old, mice.

(E–L) Golgi staining of 10-week-old wild-type (WT) and CTCF cko mice to determine dendritic and spinal morphology No changes were noticed in dendritic branching, as determined by Sholl analysis, in dentate gyrus and CA1 neurons (E–G). No changes noticed in dendrite length (H–J). There is a significant decrease in spine density in CA1, but not dentate gyrus (K and L) (CTCF cko, n = 6; WT, n = 5;*$p < 0.05$ two-tailed t test). Error bars represent SEM. Scale bar, 100 μm.

and oligodendrocytes (Qki) for CTCF-positive cells in the hippocampus (Figures 1D–1L and S1). NeuN-positive neurons displayed a significantly higher intensity for CTCF immunostaining than both astrocytes and oligodendrocytes (Figure 1M). We conclude that CTCF is abundantly expressed in the brain and is enriched in neurons.

Knockout of CTCF in Excitatory Forebrain Neurons

To determine the role of neuronal CTCF in mammalian behavior and neuronal function, we developed a cell-type-specific CTCF knockout mouse model, which lacks CTCF specifically in postmitotic excitatory forebrain neurons. To this end, we crossed floxed *CTCF* mice with mice expressing Cre recombinase under the control of the *CamKIIa* promoter (Casanova et al., 2001), producing the *CamKIIa-Cre/CTCF* (subsequently referred to as CTCF cko) strain. *CamKIIa* is expressed specifically in forebrain excitatory neurons after differentiation of the neurons into postmitotic cells and is highly expressed by postnatal day five (P5) (Bayer et al., 1999). There is also subtle expression of *CamKIIa* in a few other neuron cell types, including striatal medium spiny neurons. Immunostaining confirmed the successful knockout of CTCF expression in hippocampal neurons (Figure 2A). In addition, real-time PCR and western blot determined an ~50% decrease in CTCF levels in dissected hippocampus, which is expected due to the high cellular heterogeneity in brain tissue (Figures S2A and S2B).

The CTCF cko mice developed normally to adulthood. They were slightly underweight at the age of 5 weeks but displayed normal weight at later developmental time points (Figure 2C). However, CTCF cko mice displayed a shortened lifespan. The mice die between 14 and 17 weeks of age (Figure 2B). TUNEL and Nissl staining in the brain of 14-week-old mice revealed massive apoptosis specifically in the hippocampus (Figures 2D, S2C, and S2D), while no apoptosis is detectable at 12 weeks of age. Therefore, rapid apoptosis occurs in the hippocampus of these mice at 14 weeks of age.

We further performed Golgi staining in the hippocampus of 10-week-old mice to determine if there are any fine morphological changes in the dendritic or synaptic morphology at this time point (Figure S2E). In the granule cells of the dentate gyrus, there

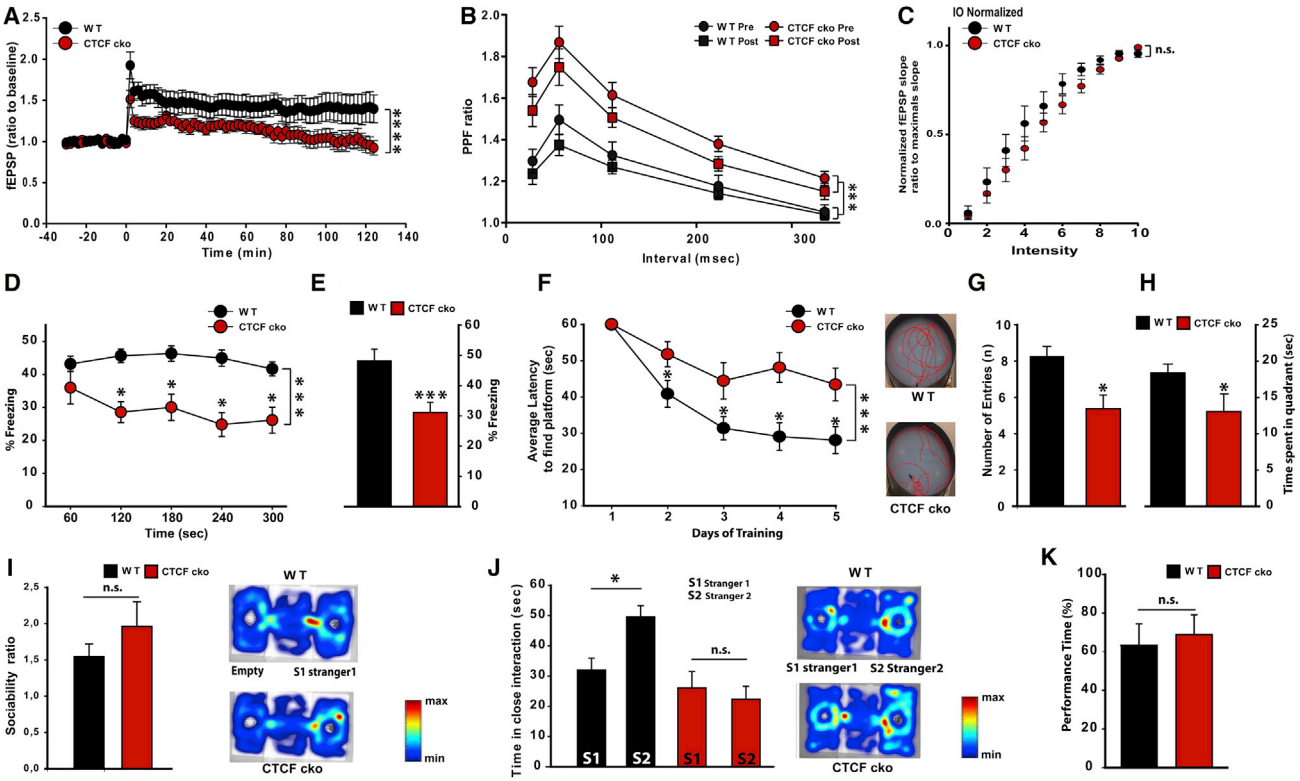

Figure 3. Deficits in Long-Term Potentiation, Spatial Memory, and Fear Memory in 10-Week-Old CTCF cko Mice

(A) Hippocampal slices from 10-week-old CTCF cko mice displayed significant LTP deficits in response to high-frequency stimulation at the Schaffer collateral synapses in the CA1 region (n = 5, $F_{77,1694} = 2.375$; ****p < 0.0001, two-way ANOVA; interaction test).

(B) Paired-pulse facilitation is altered in CTCF cko mice suggesting presynaptic neurotransmission impairment. "Pre" refers to prepotentiation, while "Post" refers to postpotentiation. (n = 5; $F_{3,44} = 11.14$; p = < 0.0001, two-way ANOVA; ***p < 0.001, Tukey test).

(C) Input/output curves of fEPSP response at the CA1 region showed no significant difference between CTCF cko mice and WT littermates.

(D and E) CTCF cko mice displayed less freezing 24 hr after training in the contextual fear conditioning test (CTCF cko, n = 14; WT, n = 12; $F_{1,1} = 79.332$, ***p < 0.001; *p < 0.05, two tailed t test) (D) and less freezing during tones in the cue-dependent fear conditioning test (***p < 0.001, two tailed t test) (E).

(F) CTCF cko mice displayed a higher latency to find a hidden platform in the Morris water maze test during five consecutive training days (CTCF cko, n = 8; WT, n = 7; $F_{1,1} = 27.376$, ***p < 0.001; *p < 0.05, two tailed t test).

(G and H) 24 hr after the last training session (probe day), the swimming pattern of WT and CTCF cko mice during the probe day; CTCF cko mice displayed fewer visits (G) to the quadrant of the arena where the hidden platform was previously located and spent less time (*p < 0.05, two-tailed t test) in that quadrant (H).

(I and J) CTCF cko mice displayed no significant dysfunction in sociability (I) and no preference toward a novel mouse in social recognition test (J) in the three-chambered social test compared to WT littermates (heatmaps of WT and CTCF cko mice during the sociability and recognition test) (CTCF cko, n = 14; WT, n = 12; *p < 0.05, two-tailed t test).

(K) CTCF cko showed no significant locomotor deficits in rotarod test (CTCF cko, n = 14; WT, n = 12).

Error bars represent SEM.

were no differences in dendritic branching, as detected by Sholl analysis, in dendrite length and in spine density (Figures 2E, 2H, and 2K). In the pyramidal cells of the CA1, there were no differences in dendritic branching or dendrite length (Figures 2F, 2G, 2I, and 2J), but there was a significant decrease in spine density (Figure 2L). Therefore, CTCF cko mice display only very subtle synaptic changes at the age of 10 weeks.

In order to determine whether CTCF deletion affects synaptic functioning, we examined a form of synaptic plasticity called long-term potentiation (LTP) in hippocampal slices derived from 10-week-old mice. CTCF cko mice showed robust LTP deficits in the Schaffer collateral synapses at the CA1 (Figure 3A). We also observed differences in paired-pulse facilitation curves of the CTCF cko, which suggest altered presynaptic functioning (Figure 3B). We did not observe a significant alteration of the baseline synaptic transmission as measured by input-output curves (Figure 3C). Together, these data suggest that CTCF is not necessary for basal synaptic function but is mandatory for LTP, the major physiological driver of learning and memory.

Behavioral Analysis of 8- to 10-Week-Old CTCF cko Mice

In light of the genetic connection between CTCF and intellectual disabilities and the deficits in long-term potentiation, we tested 8- to 10-week-old CTCF cko mice for learning and memory in two classical paradigms: fear conditioning and the Morris water maze. In the contextual fear conditioning paradigm, CTCF cko mice displayed lower freezing levels when reintroduced to the context where the mice had previously experienced

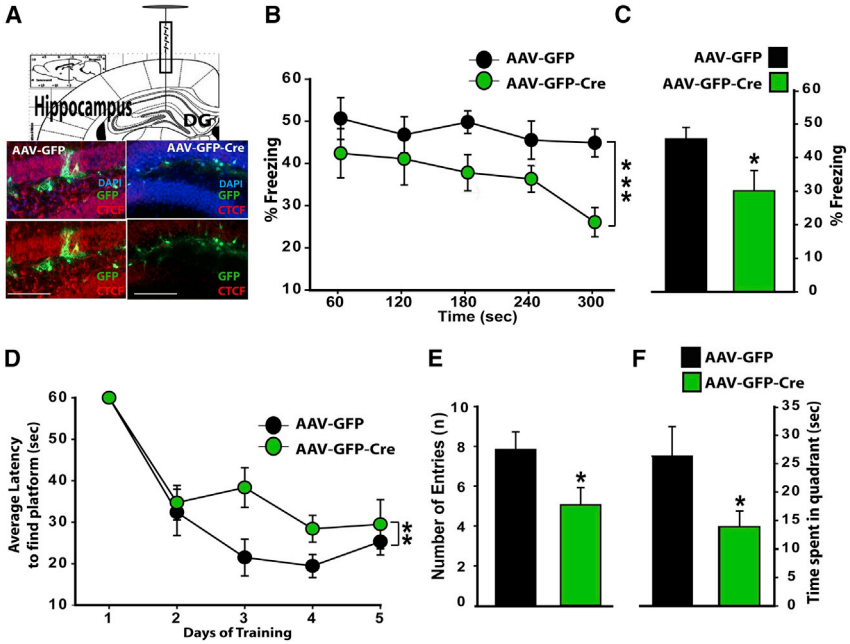

Figure 4. Virus-Mediated Knockdown of CTCF in Hippocampus Induces Deficits in Spatial Memory and Fear Memory

(A) Schematic of viral injection of either AAV-GFP or AAV-GFP-Cre into the dentate gyrus region of the hippocampus of CTCF floxed mice. Immunohistochemistry shows CTCF decreased expression at point of AAV-GFP-Cre virus injection.

(B and C) AAV-GFP-Cre injected mice displayed less freezing 24 hr after training in the contextual fear conditioning test (AAV-GFP-Cre, n = 12; AAV-GFP, n = 11; $F_{1,1} = 19.44$, ***p < 0.001, two-way ANOVA) (B) and less freezing during tones in the cue-dependent fear conditioning test (*p < 0.01, two-tailed t test) (C).

(D) AAV-GGP-Cre injected mice displayed a higher latency to find a hidden platform in the Morris water maze test during five consecutive training days (AAV-GFP-Cre, n = 12; AAV-GFP, n = 11; $F_{1,1} = 6.468$, **p < 0.01, two-way ANOVA).

(E and F) 24 hr after the last training session (probe day), AAV-GGP-Cre injected mice displayed fewer visits (E) to the quadrant of the arena where the hidden platform was previously located and spent less time (F) in that quadrant (*p < 0.05, two tailed t test). Error bars represent SEM. Scale bar, 100 μm.

a shock, indicative of decreased contextual learning (Figure 3D). In the tone-dependent cued fear conditioning paradigm, CTCF cko mice displayed lower freezing when presented with tones 1 day after pairing tones to a shock (Figure 3E), indicating a deficit in cued learning.

In the Morris water maze, another test for spatial memory, CTCF cko mice displayed a higher latency to find a hidden platform during the acquisition phase (Figure 3F), indicative of impaired spatial memory. During a probe trial, in which the hidden platform is removed from the tank, the CTCF cko mice displayed decreased number of visits and time in the platform quadrant (Figures 3G and 3H).

Sociability and social novelty recognition were examined in the three chambered social test (Moy et al., 2004). CTCF cko mice displayed normal sociability, as defined by preference for social interaction in comparison to empty chambers (Figure 3I). However, unlike wild-types, CTCF cko mice displayed no preference for being in a chamber with a novel mouse compared to a familiar mouse (Figure 3J). These results suggest a defect in social recognition, while sociability remains intact. In addition, the CTCF cko mice showed normal rotarod activity (Figure 3K), indicating normal locomotor behavior. Overall, the 8- to 10-week-old CTCF cko mice display major deficits in learning- and memory-related paradigms.

Adenoviral-Mediated Knockout of CTCF in the Hippocampus

In order to determine if a short-term, hippocampal-specific knockdown of CTCF may induce deficits in learning and memory, we used adenovirus-mediated knockout of CTCF. GFP and Cre-expressing viral particles (AAV-GFP/Cre), or GFP alone-expressing particles (AAV-GFP), were injected bilaterally into the hippocampus of floxed CTCF mice (Figures 4A, S3A, and S3B). 2 weeks after injection, mice were subjected to the fear conditioning and Morris water maze tests. In addition, TUNEL staining at 6 weeks after injection verified that CTCF ablation did not induce any cell death, therefore ruling out any effects of cell death on behavioral results (Figures S3C and S3D).

In the contextual fear conditioning test, AAV-GFP/Cre-injected mice displayed lower freezing compared to AAV-GFP-injected mice (Figure 4B). The AAV-GFP/Cre mice displayed the same deficits in the cued fear conditioning test, with less freezing during the presentation of cues in novel context (Figure 4C).

In the Morris water maze spatial memory test, there was a significant group effect for genotype where AAV-GFP/Cre-injected mice required a significantly longer time to find the hidden platform (Figure 4D). During the probe test, the AAV-GFP/Cre mice spent less time in the platform quadrant and had fewer entries into that quadrant (Figures 4E and 4F). In conclusion, these results indicate that CTCF in the hippocampus is necessary for memory formation.

Hippocampal Gene Expression after CTCF Ablation and CTCF-Binding Sites on Hippocampal Chromatin

Our next goal was to understand the molecular mechanism through which hippocampal CTCF is regulating learning and memory. First, we performed RNA sequencing (RNA-seq) to determine differentially expressed genes in 10-week-old CTCF cko hippocampus. Second, we determined the overlap between differentially expressed genes and CTCF-binding sites in the mouse hippocampus through chromatin immunoprecipitation sequencing (ChIP-seq) analysis. A total of 321 genes were downregulated in the knockout hippocampus, compared to 468 upregulated genes (false discovery rate [FDR] < 0.05) (Figure 5A; Table S1). Gene Ontology analysis for biological process and pathway revealed that downregulated genes were enriched in categories including plasma membrane adhesion molecules and cadherin signaling pathway (Figure 5B). Furthermore, a

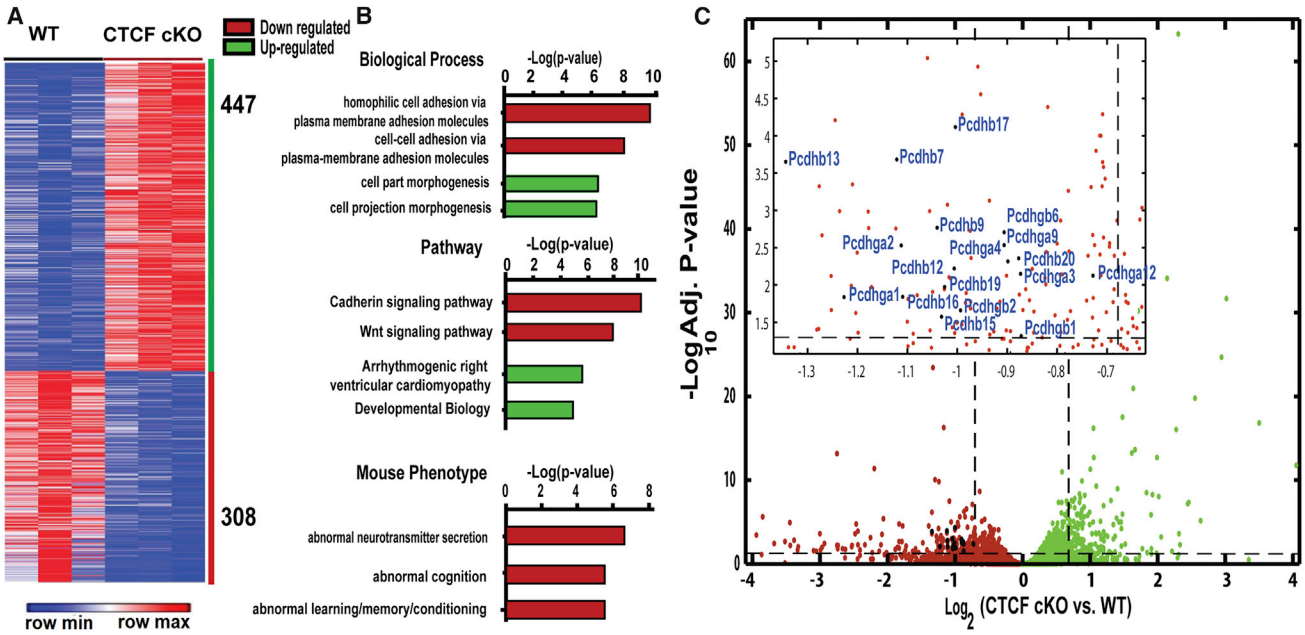

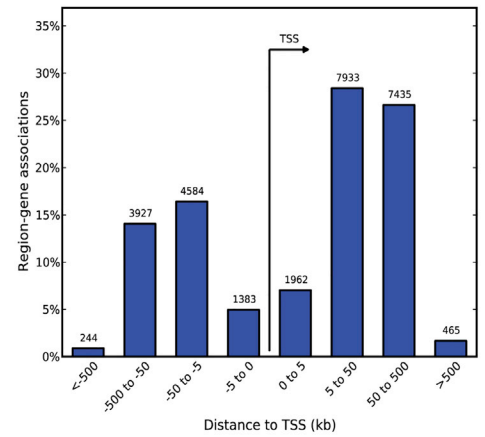

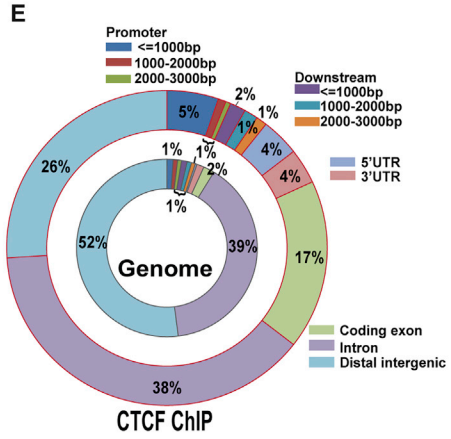

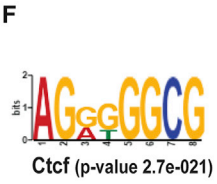

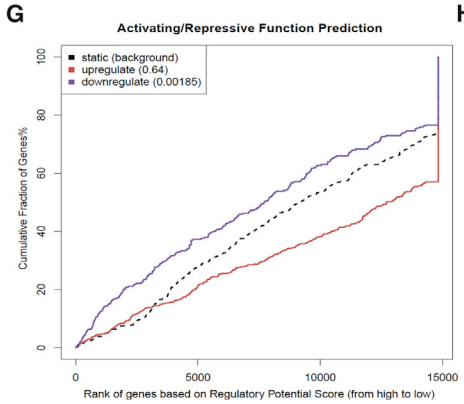

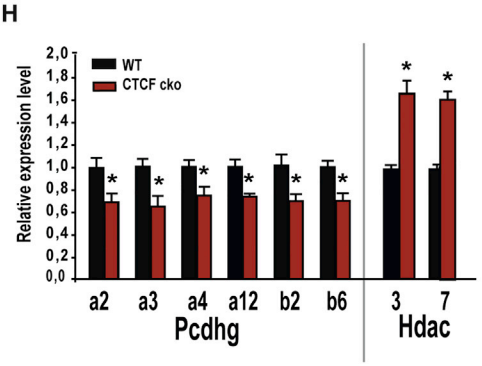

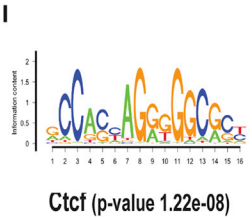

(legend on next page)

closer examination of gene expression patterns revealed that mostly protocadherin genes were significantly downregulated (Figure 5C). Importantly, protocadherins are known to be crucial for neuronal connectivity and assembly. While a previous study has shown that neuronal CTCF is responsible for protocadherin expression at earlier developmental time points (Hirayama et al., 2012), the current data determine that this role is maintained at later stages of brain development and is not restricted to in utero development. Of great interest, genes that were downregulated were also enriched for categories including abnormal cognition and abnormal learning, memory, and conditioning, suggesting that CTCF is specifically involved in the regulation of learning and memory genes. In contrast, apoptotic genes were not among the dysregulated genes.

Next we performed ChIP-seq to determine CTCF-binding sites in the hippocampal chromatin at a genome-wide level. Initial analysis by the Genomic Regions Enrichment of Annotations Tool (GREAT) revealed that CTCF peaks were spread out across the genome, both in promoter and non-promoter regions (Figure 5D; Table S2). The Cis-regulatory Element Annotation System (CEAS) identified a significant enrichment of peaks in both the promoter and coding exons (5.2% of peaks in promoters and 18% in coding exons) compared to the representation of promoters and exons in the entire genome (2% of genome are promoters and 2% of genome are coding exons) (Figures 5E and S4A). As expected, there were a higher number of CTCF sites in non-promoter regions compared to promoter regions. De novo motif analysis by Discriminative Regular Expression Motif Elicitation (DREME) identified a top motif ($p = 2.7e\text{-}21$) similar to the known CTCF-binding motif (Figures 5G and S4B). Furthermore, Genomatix analysis revealed, 9,466 out of the 15,109 significant ChIP-seq peaks contained the canonical CTCF-binding motif (Table S3).

Next, we examined whether CTCF may have a direct role in activation or repression of target genes in the hippocampus. To this end, we used Binding and Expression Target Analysis (BETA), a Bioinformatics tool that integrates ChIP-seq with differential gene expression data to identify direct target genes (Wang et al., 2013). The output is a cumulative distribution function of the gene groups (upregulated, downregulated, and non-affected genes) and uses a one-tailed Kolmogorov-Smirnov test to determine whether CTCF-binding sites were significantly enriched in the upregulated or downregulated gene sets. There was a significant enrichment of CTCF-binding sites among genes that were underexpressed in hippocampal CTCF cko mice ($p = 0.00185$) (Figure 5G). Overexpressed genes did not display an enrichment of CTCF-binding sites, suggesting that downstream effects, rather than direct CTCF binding, may be responsible for many of these differentially expressed genes. Alternatively, CTCF-mediated long-range interactions may be responsible for the repression of this gene set. Therefore, it appears that CTCF binding in genomic regions promotes local activation of gene expression. In addition, these downregulated genes display enrichment for the known CTCF-binding motif according to BETA analysis (Figure 5I; Table S4). Using real-time PCR, we verified the decreased expression of several protocadherin genes that contain CTCF-binding sites that were identified by BETA (Figure 5G; Table S4). In addition, we confirmed CTCF-binding sites in *HDAC3* and *HDAC7* (Figure S5A), two of the overexpressed genes in the knockout mice, and verified their increased expression through real-time PCR (Figure 5H). HDAC3 has previously been shown to be involved in repression of learning and memory (McQuown et al., 2011). Overall, our data verify that CTCF regulates gene expression in the mouse hippocampus, particularly in genes related to cadherin signaling and learning and memory.

Role of CTCF in Fear-Conditioning-Induced Gene Expression in the Hippocampus

Further analysis of our chromatin immunoprecipitation data revealed the existence of CTCF-binding sites in many of the classic learning and memory genes, including *Arc*, *BDNF*, *Reln*, and the memory suppressor protein *Ppp1c* (Figure 6A). Although these genes did not display differential expression in CTCF knockout hippocampus compared to wild-types, in basal conditions, it is well established that learning is dependent on activity-induced expression of these key genes. Therefore, we hypothesized that CTCF plays a role in learning-induced expression of these key genes. To this end, we performed real-time PCR to determine the hippocampal expression levels of these genes 1 hr after

Figure 5. CTCF Directly Regulates Cadherin and Cognition-Related Gene Expression

(A) Heatmap showing the 789 differentially expressed genes in the CTCF cko hippocampus compared to WT littermates (FDR adjusted p value ≤ 0.05).

(B) Gene Ontology analysis of differentially expressed genes. Enrichment of downregulated genes highlighted plasma membrane adhesion molecules, cadherin signaling pathway, abnormal cognition, and abnormal learning, memory, and conditioning.

(C) Volcano plot illustrating the distribution of differential expressed genes in hippocampus of CTCF cko mice. Each point represents up- (green) and down-regulated (red) genes in CTCF cko mice plotted against the level of statistical significance ($-\log_{10}$ adjusted p value) and fold-change ($\log_2$ (CTCF cko vs. WT). The black points indicate the set of protocadherins (*Pcdhs*) genes significantly downregulated (insert a closer view of the distribution of *Pcdhs* in downregulated gene).

(D) GREAT illustrating the genomic distribution of CTCF binding peaks with respect to transcription start site (TSS) in adult mouse hippocampus.

(E) Doughnut chart depicting the genome-wide distribution patterns of the CTCF peaks (outside circle) compared to genome background (inner circle).

(F) De novo motif analysis of CTCF peaks using the DREME program identified the top motif, which is most similar to the known CTCF-binding motif.

(G) Integration of RNA-seq and ChIP-seq data to determine CTCF direct targets genes and activator or repressive function of CTCF. The plot represents the BETA activating/repressive function of CTCF-binding target genes. Upregulated (red) and downregulated (purple) genes are plotted with respect to the non-affected genes as background (dashed line). Genes are cumulated by the rank on the basis of the regulatory potential score. Beta analysis determined a significant activation function of CTCF, as represented by the significant association of downregulated genes (in the CTCF cko mice) with CTCF-binding sites (one-tailed Kolmogorov-Smirnov test).

(H) Real-time PCR validations of both BETA and RNA-seq data of various dysregulated protocadherin genes and enriched *Hdac3* and *Hdac7* (RNA-seq only) in CTCF cko mice ($n = 6$ per group; $^*p < 0.0001$, two-tailed t test). Error bars represent SEM.

(I) A BETA motifs search in downregulated target genes showed enrichment for CTCF.

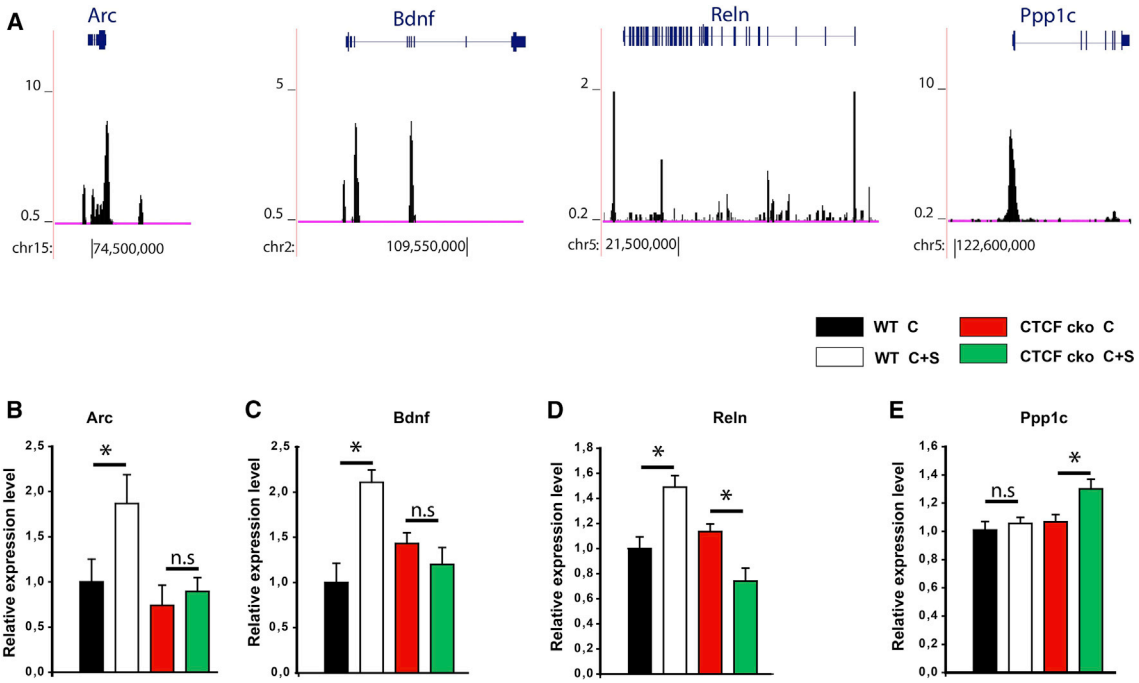

Figure 6. CTCF Is Mandatory for Fear-Conditioning-Induced Increases in Gene Expression

(A) Representative view of CTCF ChIP-seq peaks for selected learning and memory-related genes (*Arc*, *Bdnf*, *Reln*, and *Ppp1c*).

(B–E) Real-time PCR analysis of hippocampal gene expression in WT and CTCF cko animals subjected to fear conditioning. All mice were subjected to the novel environment (fear conditioning chamber), and mice were subjected to either context plus shock (C+S) or context alone (C). The pairing of context and shock increased gene expression of learning-associated genes *Arc* (n = 6 per group; $F = 5.473$; $p = 0.007$, two-way ANOVA; *$p < 0.05$, Tukey test), *Bdnf*-IV (n = 6 per group; $F = 10.391$; $p < 0.001$, two-way ANOVA; *$p < 0.05$, Tukey test), and *Reln* (n = 6 per group; $F = 13.364$; $p = 0. < 0.001$, two-way ANOVA; *$p < 0.05$, Tukey test) in wild-type mice, but not in CTCF cko animals (B–D). The pairing of context and shock increased expression of learning-suppressor gene *Ppp1c* in CTCF cko animals, but not in wild-type mice (n = 6 per group; $F = 5.311$; $p = 0.007$, two-way ANOVA; *$p < 0.05$, Tukey test) (E). Error bars represent SEM.

fear conditioning in both wild-type and knockout mice (Miller and Sweatt, 2007).

In wild-type animals, fear conditioning (context plus shock) induced an increased hippocampal expression of *Arc*, *BDNF* (promoter IV) and *Reln* compared to non-fear-conditioned animals (context only) (Figures 6B–6D). However, the pairing of context with shock had no effect on gene expression in the CTCF cko animals (Figures 6B–6D). Therefore, learning-induced expression of *Arc*, *BDNF*, and *Reln* was attenuated in CTCF cko hippocampus.

BDNF has six alternative promoters, and expression from promoter four can be upregulated by stress or learning paradigms (Martinowich et al., 2003; Lubin et al., 2008). To test if our findings are specific to promoter 4, we also performed real-time PCR on *BDNF* expressed from promoter 1 and total *BDNF*. Transcripts from total *BDNF*, but not from promoter 1, were upregulated after fear conditioning only in wild-type mice (Figure S5B). Therefore, CTCF deletion can inhibit the expression of *BDNF* specifically from promoter 4.

We also determined the gene expression pattern of *Ppp1c*, a gene involved in memory suppression (Miller and Sweatt, 2007). CTCF cko mice displayed an increase of hippocampal *Ppp1c* after fear conditioning, unlike wild-type mice, which displayed no differences in *Ppp1c* after fear conditioning (Figure 6E). Therefore, the deletion of CTCF inhibits the fear-induced expression of memory-promoting genes and promotes the expression of a memory suppressor gene.

CTCF-Dependent Chromatin Structure in the Hippocampus

To understand the high-order three-dimensional structure of the memory genes we previously examined, we first examined their structure in a previously published high-resolution Hi-C dataset (Rao et al., 2014). Several studies have already determined that CTCF regulates the three-dimensional structure of the protocadherin genes in the brain (Hirayama et al., 2012; Fukuda et al., 2008). Therefore, we focused on understanding the possible role of CTCF in the three-dimensional structure of the activity-dependent gene regulation. *BDNF* and *Arc* genes are found within large TADs that include the neighboring genes (Figure S6). However, the resolution of Hi-C does not suffice to define specific short-range interactions between the promoter and regulatory elements, including CTCF-binding sites.

Thus, we applied chromosome conformation capture combined with next-generation sequencing (4C-seq) technique to detect all the chromosomal contacts of *Arc* and *BDNF* IV promoters. We identified several chromatin contacts between the *Arc* promoter and nearby genomic regions (Figure 7A). Interestingly, two of these contacts were lost in hippocampal chromatin from CTCF cko animals. These contacts overlapped with CTCF

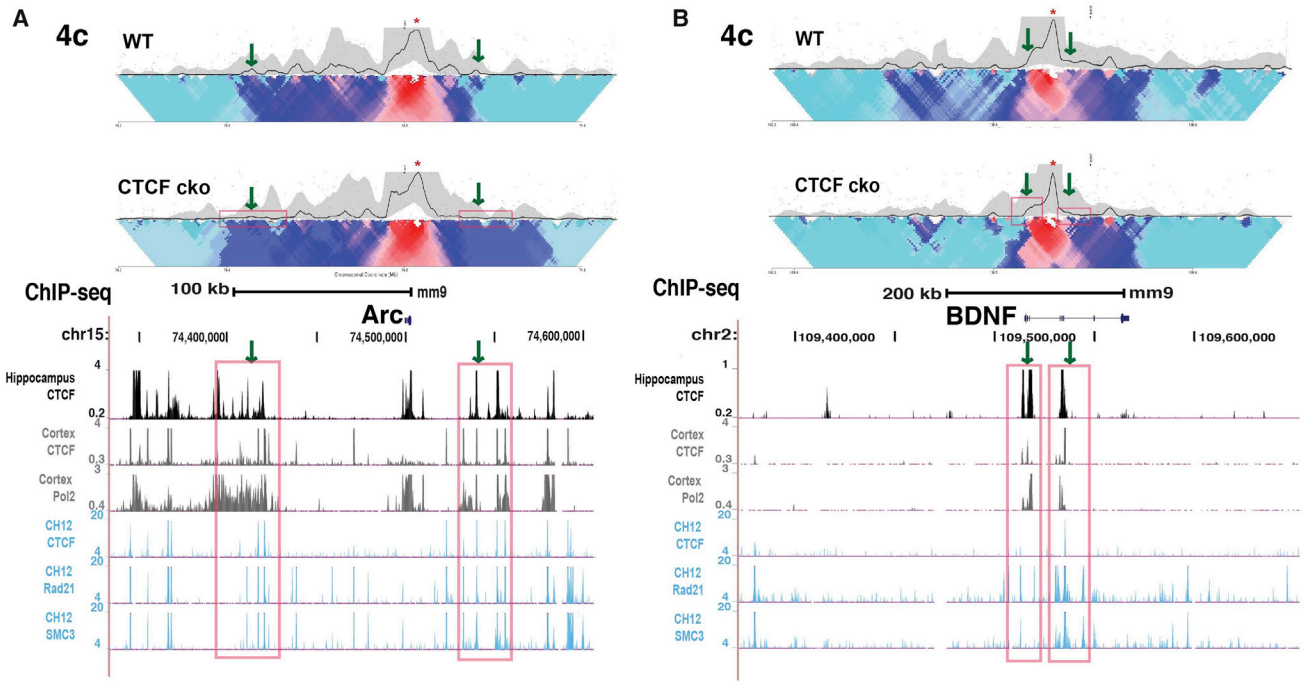

Figure 7. CTCF Regulates High-Order Chromatin Structure of *Arc* and *BDNF* Genes

(A and B) Representative view of the 4C analysis showing long-range chromosomal associations of *Arc* (A) and *BDNF* (B) gene promoters in hippocampus of WT and CTCF cko mice. UCSC genome browser tracks mapping the ChIP-seq data of hippocampus (CTCF), cortex (CTCF and Pol2), and CH12 (B cell lymphoma) (CTCF, Rad21, and SMC3) from ENCODE. Cortex and CH12 data from the mouse ENCODE project (Robertson et al., 2007). Green arrows indicate chromosomal contact loci that were diminished in the CTCF-deficient mice and overlap with a CTCF-binding site, as determined by our ChIP-seq data (n = 5–6 per group). Asterisk (*) indicates the bait sequence and Genomic mm9 coordinates were used.

peaks from our hippocampal ChIP-seq data and binding sites for CTCF, Rad21, and SMC3, as published in Encode from B cell lymphoma studies (CH12) (Cheng et al., 2014). Therefore, these peaks likely represent CTCF-dependent chromosome loops interacting with the *Arc* promoter. Measuring the chromosomal contacts with the *BDNF* IV promoter, we have also detected multiple chromatin contacts (Figure 7B). Many of the contact peaks in close proximity to the *BDNF* IV overlap with CTCF-, Rad21-, and SMC23-binding sites and are also partly diminished in hippocampal DNA from the CTCF cko. Of interest, CTCF peaks also overlapped with RNA polymerase 2 (Pol2) peaks. It has previously been shown that CTCF interacts with Pol2 and is required for activation of specific promoters (Chernukhin et al., 2007). Therefore, we have identified the existence of CTCF-dependent chromatin interactions at the promoters of *Arc* and *BDNF*, two genes that display CTCF-dependent learning-induced changes in gene expression. In summary, these results indicate that CTCF-mediated three-dimensional structure primes genes for learning-event-induced gene expression and consolidation of fear memory.

DISCUSSION

The primary aim of this study is to understand the role of neuronal CTCF in general and CTCF-mediated chromatin organization in particular in learning and memory. The present study of CTCF might reveal important information regarding the role of chromatin organization in the brain, since CTCF is the only well-defined mammalian insulator protein with the properties to form long-range chromatin loops (Zlatanova and Caiafa, 2009a).

Our initial findings of relatively high levels of CTCF expression in the brain, and in neurons in particular, suggest that CTCF has important functions in the brain. To extensively study the role of neuronal CTCF in the adult brain, we generated a conditional deletion of CTCF mainly in excitatory forebrain neurons. Surprisingly, these mice showed no striking difference in appearance, locomotion, and general behavior in home cage until they died the age of 14–17 postnatal weeks. A previously published model of CTCF depletion in neuronal precursors induced death at approximately the age of birth (Watson et al., 2014), while depletion in post-mitotic neurons induced death at ~4 weeks of age (Hirayama et al., 2012). Therefore, neither of the previous models was adequate for the study of adult mammalian behavior. In contrast to the previous models, *CamKIIa*- dependent expression of Cre occurs only in post-mitotic forebrain neurons, and expression peaks at ~P5 (Bayer et al., 1999). In the previously published Nex-Cre model, Cre is expressed at the beginning of E11.5 and is also expressed in the developing spinal cord and cerebellum (Showell and Conlon, 2007). These differences may partially explain why the previous model displayed gross motor abnormalities and severe neuronal morphological deficits at juvenile age while our current model does not (Hirayama et al., 2012).

Therefore, fully mature forebrain post-mitotic neurons can survive and function significantly longer without CTCF without inducing major morphological changes than cells at an earlier developmental stage. To our knowledge, no other cell type has been shown to survive for such long periods of time without CTCF.

At 10 weeks of age, we found no dysregulation in dendritic arborization in the hippocampus of CTCF cko mice. This underlies that no severe dysregulation of neuronal morphology at this time period. However, there is a significant decrease in dendritic spine density specifically in the CA1 region. This finding may suggest a problem in maintenance of the synaptic structure, while the developmental process of dendritic development is not affected.

In tests for cognitive abilities, both the CTCF cko mice and mice with a hippocampus-specific knockout displayed memory deficits in the Morris water maze and fear conditioning tests. The adenoviral-mediated knockdown verifies that the effects on memory are not due to long-term effects of CTCF depletion, but even a short-term depletion can affect cognitive function. In addition, these deficits in learning in memory are correlated to impaired long-term potentiation and reduced spine density in the CTCF cko model, without changes in basal synaptic transmission and dendritic arborization at this time point.

At the transcriptional level, CTCF cko hippocampi displayed a downregulation of genes involved in protocadherin signaling and learning functions. Through comparison with ChIP-seq data from the mouse hippocampus, we determined that the downregulated genes are enriched in CTCF-binding sites. In contrast, upregulated genes, which are mostly unrelated to neuronal function, are not enriched in CTCF-binding sites. Therefore, the upregulation of many of these genes are likely to be through downstream mechanisms. In the previously published Nex-Cre-mediated ablation of CTCF, the decrease in protocadherin expression was associated with severe dysregulation of dendritic morphology and arborization (Hirayama et al., 2012). In our model, dendritic morphology was not affected, with only minor deficits in spine density in the CA1 region. In addition, basal synaptic transmission was not affected. These findings suggest that the effects of CTCF on dendritic morphology and arborization are restricted to early developmental periods, before *CamKIIa* is fully expressed at P5 (Bayer et al., 1999). However, it is possible that the lack of protocadherins at these later stages may be partly responsible for subtle synaptic abnormalities that were evident in our model, including decreased spine density and decreased LTP.

CTCF cko mice display differential fear-conditioning-induced gene expression in select genes important for learning and memory, such as *BDNF* (Lubin et al., 2008), *Arc*, *Reln*, and *Ppp1c* (Miller and Sweatt, 2007). Interestingly, in these genes, CTCF cko mice did not display differential gene expression, compared to wild-type mice, at basal conditions (context only). This finding suggests the existence of a subgroup of memory-related genes for which CTCF is not necessary for basal gene expression but is necessary for activity-induced induction of gene expression. However, *Reln* levels were decreased after fear conditioning in CTCF cko animals, while they are increased in wild-type animals. In addition, we found multiple CTCF-binding sites in the *Reln* gene. This suggests a very complex regulation of *Reln* expression by CTCF, which would require further experimentation to understand. Notably, the expression of *Reln* is downregulated in the cortex of individuals diagnosed with schizophrenia (Impagnatiello et al., 1998; Juraeva et al., 2014), and SNPs in the genomic region of CTCF have been found to be associated with schizophrenia (Juraeva et al., 2014).

CTCF is a known chromatin organizer and plays a key role in mediating long-range chromatin loops between distal regulatory sequences (Splinter et al., 2006). In our study, we employed 4C chromosome capture methodology to achieve a global view on the regulation of CTCF at the locus of *Arc* and *BDNF* in WT and CTCF cko mice. Importantly, we observe novel contact points in WT mice. These contact points were found at CTCF-binding sites, as revealed by ChIP-seq analysis, and were partially diminished in the CTCF cko mice. This loss of contact specificity in CTCF cko hippocampi is in agreement with a previous Hi-C study showing that CTCF depletion, through small interfering RNA (siRNA), induced a more random three-dimensional structure (Zuin et al., 2014). Both that study and the current study suggest that CTCF restricts the chromatin contact points to specific genomic locations. We note that it is difficult to assess the exact role of each specific diminished peak in activity-dependent gene expression of *Arc* and *BDNF*. In order to address this issue, future experiments can take advantage of the clustered regularly interspaced short palindromic repeats (CRISPR) and CRISPR-associated (Cas) genome editing tool to edit these sites and examine the effect of their loss on activity-dependent gene expression and behavior.

In our hippocampal ChIP-seq data, we notice a clear overlap with the different cohesin factors. Previous studies have demonstrated that these factors work in concert with CTCF to define its chromatin-binding positions and diverse activities, including transcription activation, repression, and long-range interactions (Sofueva et al., 2013). Thus, it is likely that CTCF facilitates the activity of yet-unknown transcription factors co-occupying CTCF-binding sites by associating them with promoters of memory-related genes such as *BDNF* and *Arc*. Overall, the overlap of Pol2-, SMC3-, RAD21-, and CTCF-binding sites at a subset of the 4C peaks suggests that a CTCF-mediated high-order structure may be important for the recruitment of Pol2 to *BDNF* and *Arc* promoters (Zlatanova and Caiafa, 2009b; Chernukhin et al., 2007).

CTCF was recently found to be mutated in a subset of individuals with intellectual disabilities (Gregor et al., 2013). In addition, CTCF was found to regulate the expression of FMRP1 (Lanni et al., 2013). Epigenetic silencing of FMRP1 is the cause of fragile X syndrome, the most common form of inherited intellectual disabilities (Madrigal et al., 2012). Our study directly determines the role of CTCF in behavior and gene transcription in the brain and connects these findings to higher-order chromatin structure in the brain.

The current study determines two molecular mechanisms that may mediate the effects of CTCF on learning and memory in the brain. These mechanisms include the maintenance of basal spinal density through expression of the protocadherins and experience-dependent regulation of primary learning and memory genes. This finding should prompt many future studies, which may focus on key CTCF-binding partners that have also been

implicated in neurodevelopmental disorders, including cohesin (Zakari et al., 2015; Wendt et al., 2008) and CHD8 (Ishihara et al., 2006; O'Roak et al., 2012).

EXPERIMENTAL PROCEDURES

Mice

Mice were housed according to Federation of Laboratory Animal Science Associations (FELASA) guidelines. All mice were bred and maintained in a vivarium at 22°C in a 12-hr light/dark cycle, with food and water available ad libitum. To generate post-mitotic forebrain neuron-specific CTCF deletion mice, the *CamKIIa-Cre* line was crossed to *CTCF loxp/loxp* (floxed CTCF) mice (kindly provided by Prof. Niels Galjart, Erasmus MC). To produce the mice for all experiments, *Cre*+/floxed *CTCF* mice were bred with *Cre*−/floxed *CTCF* mice. *Cre*-negative (wild-type) and *Cre*-positive (CTCF knockout) littermate offspring were used in all experiments. All behavioral tests were performed with 8- to 10-week-old male mice. All experimental protocols were approved by the Animal Care and Use Committee of Bar Ilan University.

Contextual and Cued Fear Conditioning

1 day prior to memory training, each mouse was habituated to the fear conditioning cage for 5 min. On the training day, each mouse was placed into the conditioning chamber (10.5 × 10.5 × 10.5 cm) and allowed to explore freely for 2 min. A tone (75 dB) was sounded as the conditioned stimulus for 30 s followed by a 2-s mild foot-shock (0.7 mA) as the unconditioned stimulus. Following a 1-min break, another tone and shock was administered. The mouse was returned to the home cage 1 min after the second tone-shock pair. The next day, 24 hr after the training session, the mice were placed back into the conditioning chamber for 5 min and their freezing behavior was measured during this time period as a measure of contextual memory. 3 hr after context testing, the mice were placed into a different chamber with a novel odor, flooring, and light for cue-dependent memory testing. Following a 2-min habituation, the tone was presented thrice for 30 s with an interval of 1 min in between each tone. Freezing during the three tone periods was recorded. The EthoVision XT 10- Noldus was used to analyze the videos.

Morris Water Maze

The test was performed in a circular tank of 130 cm diameter with a hidden platform of 15 cm diameter. The tank was filled with water at 22°C ± 2°C till the platform is submerged (~1 cm below the water) and made opaque with skimmed milk powder. A single mouse was gently placed in one of the four quadrants and allowed to locate the platform in 60 s. Two trials per day were performed for 5 days with the platform in the same quadrant. Latency to reach the platform for the 5 days was recorded. On the sixth day, the probe test was conducted by removing the platform. The mice were allowed to swim for 60 s to locate the platform. The percentage of time spent in each quadrant and the number of platform crossings was recorded. EthoVision XT 10- Noldus was used to analyze the videos.

Three-Chambered Social Test

The three-chamber paradigm was performed as previously described (Kratsman et al., 2016). The three-chamber apparatus is a non-glare Perspex box (60 × 40 cm) with two gated walls that divide the apparatus to three chambers: left, center, and Right (20 × 40 cm). The test mouse was placed in the middle chamber for habituation (5 min) when the gates are closed for both side chambers. During the sociability test, the gates are opened for a period of 10 min for the test mice to explore the whole arena, with one chamber hosting a novel mouse and the other chamber empty. The social memory test, a new novel mouse was introduced to the empty chamber, and the test mouse is allowed a period of 10 min to freely interacting with either the novel or familiar mouse. Analysis of the time spent in each chamber is measured by EthoVision XT 10- Noldus.

Adenovirus Infection

8-week-old floxed CTCF mice were stereotaxically injected with 2 μL AAV-Cre/GFP (Biolabs Adeno-Cre-GFP (cat#1700)) or control AAV-GFP (Biolabs Adeno-GFP (cat#1060) at a rate of 0.2 μL/min. These viruses were a generous gift from Dr. Hava Henn (Bar Ilan University). Mice were anesthetized with isoflurane and placed on a computer-guided stereotaxic instrument (Angle Two Stereotaxic Instrument, myNeurolab; Leica Microsystems). The adenoviral vectors were delivered using a Hamilton syringe connected to a motorized nanoinjector. Vectors were injected into coordinates (relative to bregma: AP −1.9 mm, ML ±1.25 mm, and DV −2.0 mm) based on a calibration study indicating these coordinates as leading to the hippocampus in the C57BL/6 strain on our system. During the surgery period, animals were kept on a heating pad and were brought back to their home cages for post-surgery monitoring for 24 hr. The mice were allowed to rest for 2 weeks before behavioral testing. To validate the accuracy in targeting, the hippocampus immunostaining procedure was carried out as mentioned earlier.

RNA-Seq Library Preparation

Sequencing libraries were prepared using TruSeq RNA Sample Preparation Kit v2 (Illumina). Three sequencing libraries were prepared for each experimental group. Each library was prepared from a pool of hippocampal RNA from two mice; therefore, RNA-seq analysis was performed on hippocampal RNA from six wild-type and six CTCF cko mice. The 61-bp single-end sequencing was carried out on the Hiseq2500 Illumina sequencer.

Chromatin Immunoprecipitation

ChIP assay was performed according to the manufacturer's instructions described in the Magna G ChIP assay kit protocol (Millipore). Briefly, mouse hippocampus was isolated by punching with a 13G microdissection needle on each hemisphere. Hippocampi from ten mice per group were fixed in 1.5% formaldehyde and incubated for 10 min at room temperature. Cross-linked samples were sonicated using Covaris S220 System (Covaris) to produce chromatin fragments of 200–1,000 bp in size. The chromatin fragments were incubated with CTCF (Millipore) antibody and A+G Millipore beads at 4°C overnight for immunoprecipitation. The following day, the immunoprecipitated samples were treated using a 4-hr incubation with Proteinase K, and immunoprecipitated DNA was loaded on a purification column and eluted with the provided elution buffer.

4C

4C was performed as previously described (Schwartz et al., 2015; van de Werken et al., 2012). Briefly, mouse hippocampus was isolated by punching with a 13G microdissection needle on each hemisphere. Hippocampi from five to six mice per group were fixed in 1.5% formaldehyde and incubated for 10 min at room temperature. Crosslinking was stopped by adding 2.5 M glycine with incubation for 5 min at room temperature. The tissue was washed twice with cold PBS and then centrifuged for 7 min at 1,000 rpm (4°C).The pellet was resuspended in cold lysis buffer (50 mM Tris-HCL [pH 7.5], 150 mM NaCl, 5 mM EDTA, 0.5% NP-40, 1% TX-100 and 1X protease inhibitors [Sigma]) and incubated for 10 min on ice. The resuspended pellet was centrifuged for 5 min at 1,500 rpm, resuspended in buffer B (Thermo Scientific), and incubated with 0.3% SDS at 37°C for 1 hr, followed by a 1-hr incubation with the addition of 1.8% Triton X-100. Chromatin was digested with 400 U *Csp6I* (*CviQI*) (Thermo Scientific) overnight at 37°C. The following day, Csp6I was inactivated by incubating at 65°C for 20 min, and proximity ligation was performed with 100 U T4 DNA ligase (Roche) overnight at 4°C. Crosslinks were reversed by adding 30 μg proteinase K (Ambion, 2546) and incubating overnight at 65°C, followed by RNA degradation by 30 μg RNaseA (Ambion) for 45 min at 37°C. 3C DNA was purified by phenol-chloroform extraction and ethanol precipitation. For circularizing the 3C ligation junctions, the DNA was incubated with 200 U *DpnII* in D*pnII* buffer (New England Biolabs) overnight at 37°C. *DpnII* inactivation, DNA ligation, and precipitation were performed as described above. The resulting 4C DNA was purified with NucleoSpin columns (MACHEREY-NAGEL) and measured by Nanodrop. The efficiency of the enzymatic processes was evaluated by assessing differential DNA migration on agarose gel electrophoresis. A total of 3.2 μg of the 4C library from each sample was PCR-amplified using the gene promoters as viewpoints. To multiplex several experiments and conditions on the same sequencing lane, 4-bp indexes were assed to 4C oligonucleotides flanking the Csp6I recognition site. Primers sequences are listed in Table S5. PCR

was performed with Platinum hot-start taq (Invitrogen) as follows: 94°C for 2 min followed by 27 cycles of 94°C for 15 s, 60°C for 1 min, and 68°C for 3 min and a final elongation step at 68°C for 7 min.

Pooled 4C libraries were sequenced and yielded 50-bp single-end reads on the HiSeq 2000 platform. Following demultiplexing according to the index sequence, reads were analyzed using the 4C analysis pipeline (http://compgenomics.weizmann.ac.il/tanay/?page_id=367; van de Werken et al., 2012). This algorithm maps the reads to the primary (*Csp6I*) and secondary (*DpnII*) restriction enzymes locations on the reference genome (mouse mm9) and corrects for technical biases from fragment lengths and GC-content. Medians of normalized coverage for running windows ranging from 2 kb to 50 kb in size were calculated and displayed as color-coded multiscale diagrams. The results for running window of 7 kb and the 20th and 80th percentiles were smoothed and presented as black trendline.

Electrophysiology

Brains from mice at 10 weeks of age were quickly removed and placed in ice-cold cutting solution (CS) containing 110 mM sucrose, 60 mM NaCl, 3 mM KCl, 1.25 mM NaH_2PO_4, 28 mM $NaHCO_3$, 0.5 mM $CaCl_2$, 7 mM $MgCl_2$, and 5 mM glucose. Hippocampi were transversely sliced (400 μm) with a SMZ7000 vibratome (Campden Instruments). Slices were allowed to recover for 30 min at room temperature in 50:50 CS/artificial cerebrospinal fluid (ACSF) containing 125mM NaCl, 2.5 mM KCl, 1.25 mM NaH_2PO_4, 25 mM $NaHCO_3$, 25 mM D-glucose, 2 mM $CaCl_2$, and 1 mM $MgCl_2$ ACSF, followed by additional recovery for 30 min in room-temperature ACSF. After initial recovery, the slices were placed in an interface chamber, BSC1 (Scientific Systems Design) and maintained at 32°C in ACSF (2 mL/min). The slices were allowed to recover for at least an additional 120 min on the electrophysiology rig prior to experimentation. All solutions were constantly aerated with 95% O_2 and 5% CO_2. Bipolar stimulating electrodes (92:8 Pt:Y) were placed at the border of area CA3 and area CA1 along the Schaffer-Collateral pathway. ACSF-filled glass recording electrodes (3–5 MΩ) were placed in the stratum radiatum of area CA1. Basal synaptic transmission was assessed for each slice by applying gradually increasing stimuli (1–10 V), using a stimulus isolator LSIU-01(Cygnus Technology) and determining the input/output relationship. All subsequent stimuli applied to slices were equivalent to the level necessary to evoke a field excitatory postsynaptic potentials (fEPSP) that was ~40% of the maximal initial slope that could be evoked. Synaptic efficacy was continuously monitored (0.05 Hz). Sweeps were averaged together every 2 min. fEPSPs were amplified by EXT-02B amplifier (NPI Electronic) and digitized by Digidata 1440 (Molecular Devices). Analysis was performed with clampfit (Molecular Devices). A stable baseline synaptic transmission was established for at least 30 min. Slices were given high-frequency stimulation (HFS) to induce LTP using two trains of 100 Hz for 1 s, with an interval of 20 s between each train. Stimulus intensity of the HFS was matched to the intensity used in the baseline recordings. The initial slopes of the fEPSPs from averaged traces were normalized to those recorded during baseline. Two-way repeated measures (RM) ANOVAs were used for electrophysiological data analysis with $p < 0.05$ as significance criteria.

Statistical Analysis

Data were judged, and reported in figures and the figure legends, to be statistically significant when $p < 0.05$ by two-tailed, two-way ANOVA or one-way ANOVA followed by Tukey's test when appropriate. Data are presented as mean ± SEM, and the number of animals (n) is mentioned.

ACCESSION NUMBERS

The accession number for the raw data files for the ChIP-seq and RNA-seq analysis reported in this paper is GEO: GSE84176.

SUPPLEMENTAL INFORMATION

Supplemental Information includes Supplemental Experimental Procedures, five figures, and five tables and can be found with this article online at http://dx.doi.org/10.1016/j.celrep.2016.11.004.

AUTHOR CONTRIBUTIONS

D.S.S. and E.E. designed experiments, analyzed data, and wrote the manuscript. D.S.S. and S.N. carried out the molecular experiments (ChIP-seq, RNA-seq, and qPCR). D.S.S. and D.G. carried out behavior experiments, viral injection, and the histology assay. D.R. and O.H. designed and carried out the 4C experimentation. M.T. carried out bioinformatics analysis on 4C data. P.R.R. and H.K. carried out the electrophysiology experiments.

ACKNOWLEDGMENTS

We would like to acknowledge and thank the Israel National Center for Personalized Medicine at the Weizmann Institute of Science, and particularly Dr. Gilgi Friedlander, for their work and great assistance in the sequencing and bioinformatics that are outlined in this manuscript. In addition, we would like to acknowledge the Bar Ilan University Faculty of Medicine Animal Facilities staff, including Dr. Roey Lahav. We thank Anita Impagliazzo for the artwork. This work is supported by the Israel Science Foundation (grant 1047/12).

Received: November 22, 2015
Revised: September 22, 2016
Accepted: October 21, 2016
Published: November 22, 2016

REFERENCES

Bayer, K.U., Löhler, J., Schulman, H., and Harbers, K. (1999). Developmental expression of the CaM kinase II isoforms: ubiquitous γ- and δ-CaM kinase II are the early isoforms and most abundant in the developing nervous system. Brain Res. Mol. Brain Res. *70*, 147–154.

Casanova, E., Fehsenfeld, S., Mantamadiotis, T., Lemberger, T., Greiner, E., Stewart, A.F., and Schütz, G. (2001). A CamKIIα iCre BAC allows brain-specific gene inactivation. Genesis *31*, 37–42.

Chang, J., Zhang, B., Heath, H., Galjart, N., Wang, X., and Milbrandt, J. (2010). Nicotinamide adenine dinucleotide (NAD)-regulated DNA methylation alters CCCTC-binding factor (CTCF)/cohesin binding and transcription at the BDNF locus. Proc. Natl. Acad. Sci. USA *107*, 21836–21841.

Cheng, Y., Ma, Z., Kim, B.H., Wu, W., Cayting, P., Boyle, A.P., Sundaram, V., Xing, X., Dogan, N., Li, J., et al.; Mouse ENCODE Consortium (2014). Principles of regulatory information conservation between mouse and human. Nature *515*, 371–375.

Chernukhin, I., Shamsuddin, S., Kang, S.Y., Bergström, R., Kwon, Y.W., Yu, W., Whitehead, J., Mukhopadhyay, R., Docquier, F., Farrar, D., et al. (2007). CTCF interacts with and recruits the largest subunit of RNA polymerase II to CTCF target sites genome-wide. Mol. Cell. Biol. *27*, 1631–1648.

Fukuda, E., Hamada, S., Hasegawa, S., Katori, S., Sanbo, M., Miyakawa, T., Yamamoto, T., Yamamoto, H., Hirabayashi, T., and Yagi, T. (2008). Down-regulation of protocadherin-alpha A isoforms in mice changes contextual fear conditioning and spatial working memory. Eur. J. Neurosci. *28*, 1362–1376.

Gregor, A., Oti, M., Kouwenhoven, E.N., Hoyer, J., Sticht, H., Ekici, A.B., Kjaergaard, S., Rauch, A., Stunnenberg, H.G., Uebe, S., et al. (2013). De novo mutations in the genome organizer CTCF cause intellectual disability. Am. J. Hum. Genet. *93*, 124–131.

Guan, J.-S., Haggarty, S.J., Giacometti, E., Dannenberg, J.H., Joseph, N., Gao, J., Nieland, T.J., Zhou, Y., Wang, X., Mazitschek, R., et al. (2009). HDAC2 negatively regulates memory formation and synaptic plasticity. Nature *459*, 55–60.

Hirayama, T., Tarusawa, E., Yoshimura, Y., Galjart, N., and Yagi, T. (2012). CTCF is required for neural development and stochastic expression of clustered Pcdh genes in neurons. Cell Rep. *2*, 345–357.

Holwerda, S., and de Laat, W. (2012). Chromatin loops, gene positioning, and gene expression. Front. Genet. *3*, 217.

Impagnatiello, F., Guidotti, A.R., Pesold, C., Dwivedi, Y., Caruncho, H., Pisu, M.G., Uzunov, D.P., Smalheiser, N.R., Davis, J.M., Pandey, G.N., et al.

(1998). A decrease of reelin expression as a putative vulnerability factor in schizophrenia. Proc. Natl. Acad. Sci. USA *95*, 15718–15723.

Ishihara, K., Oshimura, M., and Nakao, M. (2006). CTCF-dependent chromatin insulator is linked to epigenetic remodeling. Mol. Cell *23*, 733–742.

Juraeva, D., Haenisch, B., Zapatka, M., Frank, J., Witt, S.H., Mühleisen, T.W., Treutlein, J., Strohmaier, J., Meier, S., Degenhardt, F., et al.; GROUP Investigators; PSYCH-GEMS SCZ Working Group (2014). Integrated pathway-based approach identifies association between genomic regions at CTCF and CACNB2 and schizophrenia. PLoS Genet. *10*, e1004345.

Kim, M.-S., Akhtar, M.W., Adachi, M., Mahgoub, M., Bassel-Duby, R., Kavalali, E.T., Olson, E.N., and Monteggia, L.M. (2012). An essential role for histone deacetylase 4 in synaptic plasticity and memory formation. J. Neurosci. *32*, 10879–10886.

Kratsman, N., Getselter, D., and Elliott, E. (2016). Sodium butyrate attenuates social behavior deficits and modifies the transcription of inhibitory/excitatory genes in the frontal cortex of an autism model. Neuropharmacology *102*, 136–145.

Lanni, S., Goracci, M., Borrelli, L., Mancano, G., Chiurazzi, P., Moscato, U., Ferrè, F., Helmer-Citterich, M., Tabolacci, E., and Neri, G. (2013). Role of CTCF protein in regulating FMR1 locus transcription. PLoS Genet. *9*, e1003601.

Lopez-Rios, J., Duchesne, A., Speziale, D., Andrey, G., Peterson, K.A., Germann, P., Unal, E., Liu, J., Floriot, S., Barbey, S., et al. (2014). Attenuated sensing of SHH by Ptch1 underlies evolution of bovine limbs. Nature *511*, 46–51.

Lubin, F.D., Roth, T.L., and Sweatt, J.D. (2008). Epigenetic regulation of BDNF gene transcription in the consolidation of fear memory. J. Neurosci. *28*, 10576–10586.

Madrigal, I., Rodríguez-Revenga, L., Xunclà, M., and Milà, M. (2012). 15q11.2 microdeletion and FMR1 premutation in a family with intellectual disabilities and autism. Gene *508*, 92–95.

Martinowich, K., Hattori, D., Wu, H., Fouse, S., He, F., Hu, Y., Fan, G., and Sun, Y.E. (2003). DNA methylation-related chromatin remodeling in activity-dependent BDNF gene regulation. Science *302*, 890–893.

McQuown, S.C., Barrett, R.M., Matheos, D.P., Post, R.J., Rogge, G.A., Alenghat, T., Mullican, S.E., Jones, S., Rusche, J.R., Lazar, M.A., and Wood, M.A. (2011). HDAC3 is a critical negative regulator of long-term memory formation. J. Neurosci. *31*, 764–774.

Merkenschlager, M., and Odom, D.T. (2013). CTCF and cohesin: linking gene regulatory elements with their targets. Cell *152*, 1285–1297.

Miller, C.A., and Sweatt, J.D. (2007). Covalent modification of DNA regulates memory formation. Neuron *53*, 857–869.

Miller, C.A., Campbell, S.L., and Sweatt, J.D. (2008). DNA methylation and histone acetylation work in concert to regulate memory formation and synaptic plasticity. Neurobiol. Learn. Mem. *89*, 599–603.

Moore, J.M., Rabaia, N.A., Smith, L.E., Fagerlie, S., Gurley, K., Loukinov, D., Disteche, C.M., Collins, S.J., Kemp, C.J., Lobanenkov, V.V., and Filippova, G.N. (2012). Loss of maternal CTCF is associated with peri-implantation lethality of Ctcf null embryos. PLoS ONE *7*, e34915.

Moy, S.S., Nadler, J.J., Perez, A., Barbaro, R.P., Johns, J.M., Magnuson, T.R., Piven, J., and Crawley, J.N. (2004). Sociability and preference for social novelty in five inbred strains: an approach to assess autistic-like behavior in mice. Genes Brain Behav. *3*, 287–302.

O'Roak, B.J., Vives, L., Fu, W., Egertson, J.D., Stanaway, I.B., Phelps, I.G., Carvill, G., Kumar, A., Lee, C., Ankenman, K., et al. (2012). Multiplex targeted sequencing identifies recurrently mutated genes in autism spectrum disorders. Science *338*, 1619–1622.

Phillips-Cremins, J.E., Sauria, M.E., Sanyal, A., Gerasimova, T.I., Lajoie, B.R., Bell, J.S., Ong, C.T., Hookway, T.A., Guo, C., Sun, Y., et al. (2013). Architectural protein subclasses shape 3D organization of genomes during lineage commitment. Cell *153*, 1281–1295.

Rao, S.S.P., Huntley, M.H., Durand, N.C., Stamenova, E.K., Bochkov, I.D., Robinson, J.T., Sanborn, A.L., Machol, I., Omer, A.D., Lander, E.S., and Aiden, E.L. (2014). A 3D map of the human genome at kilobase resolution reveals principles of chromatin looping. Cell *159*, 1665–1680.

Robertson, G., Hirst, M., Bainbridge, M., Bilenky, M., Zhao, Y., Zeng, T., Euskirchen, G., Bernier, B., Varhol, R., Delaney, A., et al. (2007). Genome-wide profiles of STAT1 DNA association using chromatin immunoprecipitation and massively parallel sequencing. Nat. Methods *4*, 651–657.

Schwartz, M., Sarusi, A., Deitch, R.T., Tal, M., Raz, D., Sung, M.H., Kaplan, T., and Hakim, O. (2015). Comparative analysis of T4 DNA ligases and DNA polymerases used in chromosome conformation capture assays. Biotechniques *58*, 195–199.

Showell, C., and Conlon, F.L. (2007). Decoding development in Xenopus tropicalis. Genesis *45*, 418–426.

Sofueva, S., Yaffe, E., Chan, W.C., Georgopoulou, D., Vietri Rudan, M., Mira-Bontenbal, H., Pollard, S.M., Schroth, G.P., Tanay, A., and Hadjur, S. (2013). Cohesin-mediated interactions organize chromosomal domain architecture. EMBO J. *32*, 3119–3129.

Splinter, E., Heath, H., Kooren, J., Palstra, R.J., Klous, P., Grosveld, F., Galjart, N., and de Laat, W. (2006). CTCF mediates long-range chromatin looping and local histone modification in the beta-globin locus. Genes Dev. *20*, 2349–2354.

van de Werken, H.J., Landan, G., Holwerda, S.J., Hoichman, M., Klous, P., Chachik, R., Splinter, E., Valdes-Quezada, C., Oz, Y., Bouwman, B.A., et al. (2012). Robust 4C-seq data analysis to screen for regulatory DNA interactions. Nat. Methods *9*, 969–972.

Wang, S., Sun, H., Ma, J., Zang, C., Wang, C., Wang, J., Tang, Q., Meyer, C.A., Zhang, Y., and Liu, X.S. (2013). Target analysis by integration of transcriptome and ChIP-seq data with BETA. Nat. Protoc. *8*, 2502–2515.

Watson, L.A., Wang, X., Elbert, A., Kernohan, K.D., Galjart, N., and Bérubé, N.G. (2014). Dual effect of CTCF loss on neuroprogenitor differentiation and survival. J. Neurosci. *34*, 2860–2870.

Wendt, K.S., Yoshida, K., Itoh, T., Bando, M., Koch, B., Schirghuber, E., Tsutsumi, S., Nagae, G., Ishihara, K., Mishiro, T., et al. (2008). Cohesin mediates transcriptional insulation by CCCTC-binding factor. Nature *451*, 796–801.

Zakari, M., Yuen, K., and Gerton, J.L. (2015). Etiology and pathogenesis of the cohesinopathies. Wiley Interdiscip. Rev. Dev. Biol. *4*, 489–504.

Zlatanova, J., and Caiafa, P. (2009a). CCCTC-binding factor: to loop or to bridge. Cell. Mol. Life Sci. *66*, 1647–1660.

Zlatanova, J., and Caiafa, P. (2009b). CTCF and its protein partners: divide and rule? J. Cell Sci. *122*, 1275–1284.

Zuin, J., Dixon, J.R., van der Reijden, M.I., Ye, Z., Kolovos, P., Brouwer, R.W., van de Corput, M.P., van de Werken, H.J., Knoch, T.A., van IJcken, W.F., et al. (2014). Cohesin and CTCF differentially affect chromatin architecture and gene expression in human cells. Proc. Natl. Acad. Sci. USA *111*, 996–1001.